

---

# Towards a General GNN Framework for Combinatorial Optimization

---

**Frederik Wenkel\***

Department of Mathematics and Statistics  
Université de Montréal  
Mila – Quebec AI Institute  
Montreal, QC, Canada  
frederik.wenkel@umontreal.ca

**Semih Cantürk\***

DIRO, Université de Montréal  
Mila – Quebec AI Institute  
Montreal, QC, Canada  
semih.canturk@umontreal.ca

**Michael Perlmutter†**

Department of Mathematics  
Boise State University  
Boise, ID 83725  
mperlmutter@boisestate.edu

**Guy Wolf†**

Department of Mathematics and Statistics  
Université de Montréal  
Mila – Quebec AI Institute  
Montreal, QC, Canada  
guy.wolf@umontreal.ca

## Abstract

Graph neural networks (GNNs) have achieved great success for a variety of tasks such as node classification, graph classification, and link prediction. However, the use of GNNs (and machine learning more generally) to solve combinatorial optimization (CO) problems is much less explored. Here, we introduce a novel GNN architecture which leverages a complex filter bank and localized attention mechanisms designed to solve CO problems on graphs. We show how our method differentiates itself from prior GNN-based CO solvers and how it can be effectively applied to the maximum clique, minimum dominating set, and maximum cut problems in a self-supervised learning setting. In addition to demonstrating competitive overall performance across all tasks, we establish state-of-the-art results for the max cut problem.

## 1 Introduction

Recent years have seen the rapid development of neural networks for graph structured data [Wu et al., 2022, Abadal et al., 2021]. Indeed, graph neural networks (GNNs) achieve state of the art performance for tasks such as node classification and are incorporated in industrial applications such as helping power Google Maps [Derrow-Pinion et al., 2021] and Amazon’s recommender system [Wang and Ioannidis, 2022]. Popular message-passing neural networks (MPNNs) typically consider a graph together with a collections of features associated to each node [Kipf and Welling, 2016, Xu et al., 2018, Velickovic et al., 2017]. In each layer, they first perform a local aggregation which effectively smooths the features over neighboring nodes of the graph, and then perform a transformation which learns combinations of the smoothed node features.

Here, we consider the problem of developing GNNs to solve combinatorial optimization (CO) problems, a somewhat less explored yet emerging application area of graph learning. In particular, we focus on the problems of finding (i) the maximum clique, i.e., the largest fully connected subgraph,

---

\*Equal contribution.

†Equal senior author contributions.

(ii) the minimum dominating set, i.e., the smallest subset of the vertices which “dominates” the graph in the sense that every vertex is within at most one hop of the dominating set, and (iii) the maximum cut, i.e., a partition of the vertices into two clusters with as many cross-cluster edges as possible.

Notably, these tasks differ significantly from, e.g., node classification in several important ways. The aggregations used in common message passing neural networks are localized averaging operations which can be interpreted as low-pass filtering. In this manner, they effectively treat smoothness as an inductive bias. While this is a useful heuristic on homophilic social networks such as the ubiquitous CORA, CITESEER, and PUBMED datasets [Bojchevski and Günnemann, 2018], we find that this assumption is not appropriate for combinatorial problems. Moreover, in combinatorial problems, it is not reasonable to assume the presence of informative node features. Instead, algorithms are expected to learn directly from the network geometry (taking initial inputs to be constant or features derived from the graph-structure, e.g., vertex degree). Additionally, we also note that the CO problems we are interested in are typically NP-Hard. Therefore, it is computationally intractable to obtain labeled data and we must instead develop self-supervised methods. As we shall see below, this necessitates a custom loss function suited for each task of interest.

To address these challenges, we propose a novel hybrid GNN architecture which uses a sophisticated filter bank of both low-pass, localized averaging filters (analogous to standard message-passing neural networks), as well as band-pass wavelet filters which capture more intricate aspects of the network geometry. In order to balance the importance of these different filters, we use a localized attention mechanism which may choose to lend more importance to different filters on a node-by-node basis. Notably, our network builds on the design proposed in Wenkel et al. [2022] which showed that multi-filter GNNs were effective for generating solutions to the maximum clique problem [Min et al., 2022]. We compare our method to various competing methods, such as heuristics, commercial solvers, other specialized GNN-based approaches [Karalias and Loukas, 2020] and recent advances that apply GFNs to the above mentioned problems [Zhang et al., 2023]. We additionally benchmark several standard GNN variants [Kipf and Welling, 2016, Xu et al., 2018, Velickovic et al., 2017, Brody et al., 2021] as a comparison to our hybrid setup. In order to train our networks, we use custom loss problems for each task of interest. Our main contributions are:

1. We develop a novel GNN architecture with a sophisticated filter bank and a localized attention mechanism that is particularly suited for solving CO problems.
2. We evaluate our method on a variety of graph-CO problems on synthetic graph benchmarks, and demonstrate that our architecture is highly performant.
3. We prove a theorem which helps us understand the improved performance of our method relative to a closely related method in previous work.

## 2 Background: Deep learning for combinatorial optimization

Many well-known graph CO problems, including the ones we consider here, are either NP-hard or even NP-complete [Karp, 1972]. Therefore, it is impossible to efficiently generate exact solutions for large graphs. Instead, one may hope to efficiently generate *approximate solutions*. Recently, there has been increasing interest in achieving this goal via graph neural networks (GNNs) recently (although Hopfield and Tank [1985] had first proposed the idea of applying deep neural networks to CO problems nearly forty years ago). Indeed, GNNs are a natural candidate because of their success on a wide variety of tasks such as node classification, graph classification, and link prediction [Abadal et al. [2021], Wu et al. [2022]]. In the context of CO, researchers have explored ways to solve a variety of graph-CO problems using both supervised and self-supervised methods as well as reinforcement learning (RL). Unfortunately, supervised methods are often computationally infeasible due to the cost of generating labeled data for such NP-hard or NP-complete problems. RL-based solutions, on the other hand, may run into problems that arise from the large size of the state space to be explored. Therefore, we view self-supervised learning as the most promising family approaches.

Notably, Tönshoff et al. [2019], Karalias and Loukas [2020], Min et al. [2022] have all used GNNs to solve CO problems in a self-supervised setting. Tönshoff et al. [2019] solves binary constraint satisfaction problems using message-passing with recurrent states. Subsequently, Karalias and Loukas [2020] proposed a seminal self-supervised learning framework in which a GNN outputs a Bernoulli distribution over the vertex set of the input graph, and a surrogate loss function is designed to

encourage certain properties in the distribution (e.g., vertices that are assigned high probabilities form a clique) and softly enforce constraints in a differentiable manner. They then propose specific loss instantiations to tackle maximum clique and graph partitioning problems. A similar loss is derived in Min et al. [2022], who use the graph scattering transform to obtain promising results for the maximum clique problem. A notable difficulty associated with these methods is that the self-supervised loss functions are highly non-convex. This motivated a separate line of work, Sun et al. [2022] which design an annealed optimization framework that aims to optimize GNNs effectively for such loss functions. We also note the recent work by Zhang et al. [2023], which applied generative flow networks [Bengio et al., 2021] to solve CO problems in an iterative manner.

Among these works, our work is most closely related to Karalias and Loukas [2020] and Wenkel et al. [2022], relying on the same or closely related self-supervised loss functions, while improving on the learned part of the pipeline, leveraging a more powerful hybrid GNN architecture.

### 3 Problem Setup

The purpose of this paper is to develop methods for (approximately) solving combinatorial optimization problems on graphs in a scalable and computationally efficient manner.

Throughout this paper, we will let  $G = (V, E)$  denote a weighted, connected, undirected graph and assume an arbitrary (but fixed) ordering on the vertices  $V = \{v_1, \dots, v_n\}$ . In a slight abuse of notation, if  $\mathbf{x}$  is a function defined on the vertices  $V$ , we will not distinguish between  $\mathbf{x}$  and the vector defined by  $x_i = \mathbf{x}(v_i)$ . We will let  $\mathbf{A}$  be the adjacency matrix of  $G$  and let  $\mathbf{D}$  be corresponding diagonal degree matrix,  $\mathbf{D} = \text{diag}(\mathbf{A}\mathbf{1})$ . We will let  $\mathbf{X}$  denote an  $n \times F$  matrix of node features. We will let  $\mathbf{S}$  denote a graph shift operator, i.e., a matrix where  $S_{i,j} = 0$  unless  $\{v_i, v_j\} \in E$  or  $i = j$ . For example, we may choose  $\mathbf{S}$  to be the adjacency matrix  $\mathbf{A}$ , the (possibly normalized) graph Laplacian  $\mathbf{L}$ , the lazy random walk matrix  $\mathbf{P} = \frac{1}{2}(\mathbf{I} + \mathbf{A}\mathbf{D}^{-1})$ , or the matrix  $\hat{\mathbf{A}} = (\mathbf{D} + \mathbf{I})^{-1/2}(\mathbf{A} + \mathbf{I})(\mathbf{D} + \mathbf{I})^{-1/2}$  utilized in the (GCN) [Kipf and Welling, 2016].

Here, we will consider the following CO problems:

1. **Maximum Cut:** Here, the goal is to find a partition of the vertex set  $V = S \sqcup T$  that maximizes the number of edges between  $S$  and  $T$ , i.e.,  $|\{\{v_i, v_j\} \in E : v_i \in S, v_j \in T\}|$ .
2. **Maximum Clique:** In the maximum clique problem, the goal is to find a clique (i.e., a fully connected subgraph) with as many vertices as possible.
3. **Minimum Dominating Set:** A subset of the vertices  $S \subseteq V$  is called a *dominating set* if for every vertex  $v_i$  is either an element of  $S$  or a neighbor of  $S$ , in the sense that  $\{v_i, v_j\} \in E$  for some  $v_j \in S$ . Our goal here is to find a dominating set with as few vertices as possible.

## 4 Methodology

We treat each of the CO problems as a self-supervised learning problem. Our approach is based on using a GNN, described in detail in Section 5, to generate a function / vector  $\mathbf{p}$  whose  $i$ -th entry  $p_i = \mathbf{p}(v_i)$  is interpreted as the probability that  $v_i$  is in the set of interest. Our network applies a sigmoid in its finally layer ensuring that all entries are between 0 and 1. Based on  $\mathbf{p}$ , we then use a *rule-based decoders* construct a candidate solution by subsequently adding nodes ordered by decreasing probability. In the following subsections, we will explain how to develop suitable loss functions and decoders for each problem of interest.

### 4.1 Maximum Cut

In this problem, we aim to find the maximum cut  $V = S \sqcup T$ , and without loss of generality, we choose  $p_i$  to be the probability that  $v_i \in S$ . We then define  $\mathbf{y} := 2\mathbf{p} - \mathbf{1}_n$  (where  $\mathbf{1}_n \in \mathbb{R}^n$  is the vector of all 1's) so that the entries of  $\mathbf{y}$  lie in  $[-1, 1]$  (rather than  $[0, 1]$ ) and use the loss function

$$L(\mathbf{y}) := \frac{1}{2} \mathbf{y}^\top \mathbf{A} \mathbf{y} = \sum_{\{v_i, v_j\} \in E} y_i y_j. \quad (1)$$

After learning  $\mathbf{y}$ , we then set  $S$  to be the set of vertices where  $\mathbf{y}$  greater than or equal to zero and  $T$  to be the set of vertices where  $\mathbf{y}$  is negative. Intuitively, we note that every edge that connects two

nodes in different parts of the cut, i.e.,  $\text{sgn}(\mathbf{y}_i) = -\text{sgn}(\mathbf{y}_j)$ , decreases the loss, while opposite case yields a additive term that increases the loss. For example, if  $\mathbf{p} = \mathbf{1}_S$ , we have  $\mathbf{y} = \mathbf{1}_S - \mathbf{1}_T$ , and our loss function is equal to the number of cuts minus the number of intra-cluster edges. Thus, the loss function encourages a node labeling that cuts as many edges as possible.

## 4.2 Maximum Clique

For the maximum clique, we let  $\bar{\mathbf{A}}$  denote the adjacency matrix of the complement graph  $\bar{G} = (V, E^c)$ , where  $E^c$  is the set of all  $\{\{v_i, v_j\} \notin E, i \neq j\}$  and use the two-part loss function considered in Min et al. [2022] (see also Karalias and Loukas [2020]):

$$L(\mathbf{p}) := L_1(\mathbf{p}) + \beta L_2(\mathbf{p}) = -\mathbf{p}^T \mathbf{A} \mathbf{p} + \beta \mathbf{p}^T \bar{\mathbf{A}} \mathbf{p}. \quad (2)$$

To understand this loss function, consider the idealized case where  $\mathbf{p} = \mathbf{1}_S$  is the indicator function of some set  $S$ , i.e.,  $p_i = 1$  if  $v_i \in S$ ,  $p_i = 0$  otherwise. In that case, one may verify that

$$-L_1(\mathbf{1}_S) = \mathbf{1}_S^T \mathbf{A} \mathbf{1}_S = \sum_{i,j} A_{i,j} (\mathbf{1}_S)_i (\mathbf{1}_S)_j$$

is the number edges between elements of  $S$ . Similarly, see have that

$$L_2(\mathbf{1}_S) = \mathbf{1}_S^T \bar{\mathbf{A}} \mathbf{1}_S = \sum_{i,j} \bar{A}_{i,j} (\mathbf{1}_S)_i (\mathbf{1}_S)_j$$

is the number of "missing edges" within  $S$ , i.e., the number of  $\{v_i, v_j\} \in E^c, v_i, v_j \in S$ . Therefore, in minimizing  $L(\mathbf{p})$ , we aim to find a subset with as many connections, and as few missing connections, as possible. The hyper-parameter  $\beta$  is used to balance the contributions of  $L_1$  and  $L_2$ .

After computing  $\mathbf{p}$ , we then reorder the vertices  $\{v_i\}_{i=1}^n \rightarrow \{v'_i\}_{i=1}^n$  so in the new ordering  $\mathbf{p}(v'_i) \geq \mathbf{p}(v'_{i+1})$ . We then build an initial clique by initializing  $C^{(1)} = \{v'_1\}$  and iterating over  $i$ . At each step, if  $C^{(1)} \cup \{v'_i\}$  forms a clique, we add  $v'_i$  to  $C^{(1)}$ , otherwise we do nothing. Note that  $C^{(1)}$  is guaranteed to be a clique by construction.

We then repeat this process multiple times to construct additionally cliques  $C^{(2)}, \dots, C^{(K)}$ . However, on the  $k$ -th iteration, we initialize with  $C^{(k)} = \{v'_k\}$  and automatically exclude  $v'_1, \dots, v'_{k-1}$  from  $C^{(k)}$ . When then choose the maximal clique  $C^*$  to be the  $C^{(k)}$  with largest cardinality. We note that while increasing  $K$  does increase the computational cost of our decoder; however, running the decoder with different initializations  $\{v'_k\}$  is straight-forward to be parallelized.

## 4.3 Minimum Dominating Set

For the minimum dominating set problem, we use the loss function:

$$L(\mathbf{p}) := L_1(\mathbf{p}) + \beta L_2(\mathbf{p}) := \|\mathbf{p}\|_1 + \beta \sum_{v_i \in V} \exp \left( \sum_{v_j \in \mathcal{N}_{v_i}} \log(1 - \mathbf{p}(v_j)) \right). \quad (3)$$

where  $\mathcal{N}_v$  denotes the set of nodes within distance one of  $v$  (including  $v$  itself). The first loss term promotes sparsity of the dominating set. To understand the second term, note as soon as there is at least one  $v_j \in \mathcal{N}_{v_i}$  with  $\mathbf{p}(v_j) \approx 1$  we will have  $\sum_{v_j \in \mathcal{N}_{v_i}} \log(1 - \mathbf{p}(v_j)) \approx 0$ . Indeed, we note that if  $\mathbf{p} = \mathbf{1}_S$  is the indicator function of a dominating set  $S$ , we have that

$$\exp \left( \sum_{v_j \in \mathcal{N}_{v_i}} \log(1 - \mathbf{p}(v_j)) \right) = \exp(-\infty) = 0,$$

for all  $v_i$ . Therefore,  $L(\mathbf{1}_S) = \|\mathbf{1}_S\|_1$  is exactly the cardinality of  $S$ .

After learning  $\mathbf{p}$  we construct our proposed minimum dominating step in a manner analogous to the max clique case. We again begin by reordering the vertices so that  $\mathbf{p}(v'_i) \geq \mathbf{p}(v'_{i+1})$ . We then initialize our first dominating set  $S^{(1)} = \{v'_1\}$  and iterate over  $i$ . At each step, we check if  $S$  is a dominating step. If so, we stop. Otherwise, we add  $v'_{i+1}$  to  $S^{(1)}$  and repeat the process. Similarly to the maximum clique, we repeat this process several times, where we initialize  $S^{(k)} = \{v'_k\}$  (automatically excluding  $v'_1, \dots, v'_{k-1}$  from the set  $S^{(k)}$  considered on the  $k$ -th iteration) and take  $S^*$  to be the smallest dominating step  $S^{(k)}$  found in any iteration.

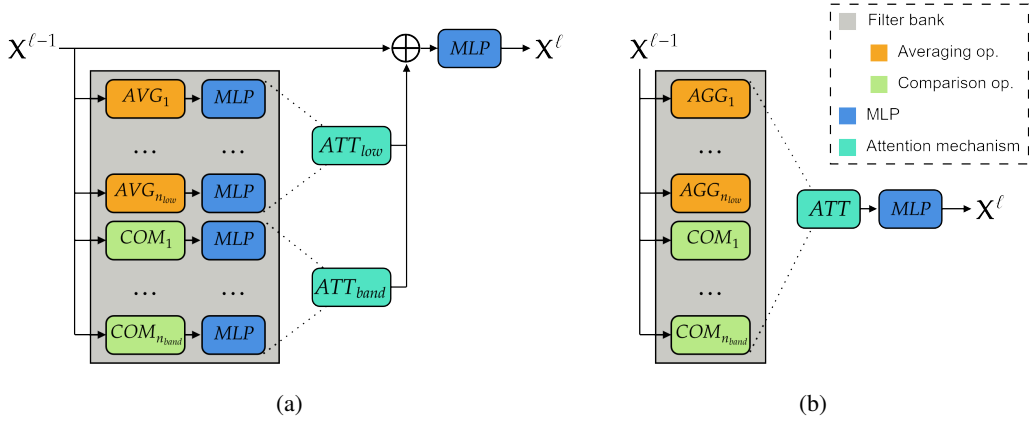


Figure 1: Illustration of the layer-wise update for (a) the new decoupled filter bank and (b) the original (non-decoupled) filter bank.

## 5 Architecture

We propose a hybrid GNN that utilizes several different types of filters including localized aggregations such as those commonly used in message-passing neural networks (which may be interpreted as low-pass filters) as well as band-pass wavelet filters such as those used in the geometric scattering transform [Gao et al., 2019, Gama et al., 2018, Zou and Lerman, 2020] which extract multiscale geometric information. The different filters are combined using a localized attention mechanism that allows the network to focus on different filters at each node in each hybrid block. This makes the architecture fundamentally different from many traditional GNN methods that apply the same aggregation at each node of the graph. Notably, our architecture is similar to that of Wenkel et al. [2022] and Min et al. [2022], but utilizes a different attention mechanism as discussed in Section 5.3.

The most basic component of our filter bank is a traditional one-step aggregation similar to popular message passing neural networks [Kipf and Welling, 2016, Hamilton et al., 2017], that has the form  $F_1(\mathbf{X}) := m(\mathbf{S}\mathbf{X})$ , where  $\mathbf{S}$  is a graph-shift operator. Further,  $m := m_{\sigma, \theta}$  is a linear layer or multi-layer perceptron (MLP) with activation function  $\sigma$  and learned weights  $\theta$ . At each node, this process *averages* information from all direct neighbors of the node, followed by a transformation step which learns new cross-feature combinations. Networks utilizing this setup are commonly referred to as *aggregate-transform* GNNs [Xu et al., 2018] due to the alternation of *aggregations* ( $\mathbf{X} \rightarrow \text{AGG}(\mathbf{X}) := \mathbf{S}\mathbf{X}$ ) and *transformations* of node features ( $\mathbf{S}\mathbf{X} \rightarrow m(\mathbf{S}\mathbf{X})$ ). Further components of our filter bank are generalizations of this filter to higher-order aggregations, that *average* information from neighbors that are  $k \geq 1$  or less apart from the central node. This can be written as

$$F_k(\mathbf{X}) := m(\mathbf{S}^k \mathbf{X}). \quad (4)$$

We note that  $F_k$  is similar to  $F_1$ , but features higher-order aggregations  $\mathbf{X} \rightarrow \mathbf{S}\mathbf{X}$ . Finally, we add filters inspired by diffusion wavelets [Coifman and Maggioni, 2006] that calculate the difference of two different aggregations  $F_{k_1}, F_{k_2}$ , where  $k_1 \neq k_2$ , by setting

$$F_{k_1, k_2}(\mathbf{X}) := m((\mathbf{S}^{k_1} - \mathbf{S}^{k_2}) \mathbf{X}). \quad (5)$$

Filters of this form are fundamentally different from the previously discussed ones as they constitute band-pass filter rather than the predominant low-pass filters in most GNN methods. They detect changes across scales by *comparing* averages of node features between two neighborhoods of different sizes.

These filters are inspired by the geometric scattering transform [Zou and Lerman, 2020, Gao et al., 2019, Perlmutter et al., 2023], a handcrafted multilayer network, which iteratively filters the input node features via diffusion wavelets [Coifman and Maggioni, 2006] of the form  $\mathbf{S}^{2^{j-1}} - \mathbf{S}^{2^j}$ , and takes vertex-wise absolute values in between wavelet filterings. Notably, the original versions of the geometric scattering transform were pre-designed feature extractors. However, subsequently, Wenkel

et al. [2022] and Tong et al. [2022] used the geometric scattering transform as a basis for a fully learned graph neural network, where Tong et al. [2022] aimed to learn the optimal diffusion scales (i.e., the powers  $k_i$  to which  $\mathbf{S}$  is raised) and Wenkel et al. [2022] introduced a *hybrid-scattering network* that combined aspects of geometric scattering and more common message passing neural networks. Since the operation  $\mathbf{X} \rightarrow (\mathbf{S}^{k_1} - \mathbf{S}^{k_2})\mathbf{X}$  compares aggregations at two different scales, we will refer to this as a *Comparison Operation*.

## 5.1 Original hybrid layer

In the architecture proposed in Min et al. [2022] (illustrated in Figure 1(b)), the input features  $\mathbf{X}^{\ell-1}$  of the  $\ell$ -th layer are filtered by each filter from a filter bank  $\mathcal{F}$  that decomposes into low-pass and band-pass filters  $\mathcal{F} = \mathcal{F}_{\text{low}} \cup \mathcal{F}_{\text{band}}$ . The filter responses are derived according to Equation 4 and 5. However, the operation  $m$  is *not* learned, and instead just set to an activation  $m(x) := \sigma(x)$  or the identity mapping  $m(x) := x$ .

Next, an attention mechanism determines the importance of information of different filters for each individual node. For each filter response  $\mathbf{H}_f := F(\mathbf{X}) \in \mathbb{R}^{n \times d}$  of  $F \in \mathcal{F}$ , and transformed input features  $\mathbf{H} := \mathbf{X}\mathbf{W}$ , this takes the form

$$\mathbf{s}_f := \sigma([\mathbf{H} \parallel \mathbf{H}_f] \mathbf{a}) \in \mathbb{R}^{n \times 1}, \quad (6)$$

where  $\parallel$  denotes horizontal concatenations. The softmax is applied to normalize importance scores across channels, resulting in a normalized score  $\bar{\mathbf{s}}_f \in \mathbb{R}^n$  where

$$\bar{\mathbf{s}}_f(v) = \text{softmax}(\{\mathbf{s}_f(v) : f \in \mathcal{F}\}). \quad (7)$$

Importantly, we note that each  $\mathbf{s}_f$  and  $\bar{\mathbf{s}}_f$  will take different values for each node. Therefore, it acts as a localized attention mechanism, which can up-weight different filters at different graph regions. Next, the filter responses are re-weighted according to the attention scores, yielding a *hybrid representation*  $\mathbf{H}_{\mathcal{F}} \in \mathbb{R}^{n \times d}$ , where

$$\mathbf{H}_{\mathcal{F}} = \sum_{f \in \mathcal{F}} (\bar{\mathbf{s}}_f \circ \mathbf{1}_d) \odot \mathbf{H}_f. \quad (8)$$

Here,  $\circ$  and  $\odot$  denote the outer and Hadamard product, respectively. The final output of each block is now generated by applying an MLP to the hybrid representation, i.e.,

$$\mathbf{X}^{\ell} := \text{MLP}(\mathbf{H}_{\mathcal{F}}). \quad (9)$$

## 5.2 Proposed novel layer with decoupled filter bank

We propose to separate our filters into two filter banks as illustrated in Figure 1(a), where  $\mathcal{F}_{\text{low}}$  denotes the set of all low-pass filters (as in Equation 4) and  $\mathcal{F}_{\text{band}}$  denotes the set of band-pass filters (as in Equation 5).

Our first important modification is that we use *learned* filters in Equation 4 and 5 with an individual operation  $m_{\sigma, \theta} := m_{\text{id}, \mathbf{W}}$  for each, where  $\mathbf{W} \in \mathbb{R}^{n \times d}$  is learned. This is important as low-pass and band-pass filters are fundamentally different, making the indirect weight sharing in Equation 9 challenging (recall that  $\mathbf{H}_{\mathcal{F}}$  is a different weighted sum over the filter responses at every node). Intuitively *averaging* features from a node neighborhood versus *comparing* node features of two differently-sized neighborhoods, respectively.

Similar to Equation 6-8, we apply an attention mechanism that determines each channel’s importance for each individual node. However, the normalization of importance scores (Equation 7) is *decoupled*, i.e., carried out separately for low-pass and band-pass channels, yielding normalized score vectors  $\bar{\mathbf{s}}^{\text{low}}, \bar{\mathbf{s}}^{\text{band}} \in \mathbb{R}^{n \times d}$ .

Accordingly, the filter responses are also re-weighted separately, yielding *hybrid representations*  $\mathbf{H}_{\mathcal{F}_{\text{low}}}, \mathbf{H}_{\mathcal{F}_{\text{band}}} \in \mathbb{R}^{n \times d}$ , where

$$\mathbf{H}_{\mathcal{F}_{\text{low}}} = \sum_{f \in \mathcal{F}_{\text{low}}} (\bar{\mathbf{s}}_f^{\text{low}} \circ \mathbf{1}_d) \odot \mathbf{H}_f, \quad (10)$$

for the lowpass filters and analogous for the bandpass filters.

Finally, we modify Equation 9 by applying an MLP to the summation of the input node features and the hybrid representations, i.e.,

$$\mathbf{X}^{\ell} = \text{MLP}(\mathbf{X}^{\ell-1} + \mathbf{H}_{\mathcal{F}_{\text{low}}} + \mathbf{H}_{\mathcal{F}_{\text{band}}}). \quad (11)$$

This adds a filter-dependent bias to the input features  $\mathbf{X}^{\ell-1} \rightarrow \mathbf{X}^{\ell-1} + \mathbf{B}$  with  $\mathbf{B} := \mathbf{H}_{\mathcal{F}_{\text{low}}} + \mathbf{H}_{\mathcal{F}_{\text{band}}}$ , which allows each filter  $f \in \mathcal{F}$  to learn an individual bias to the input node features, weighted at the node level by the attention mechanism.

### 5.3 Making sense of the proposed layer

We recall that the novel attention mechanism introduced above builds upon a class of attention mechanisms utilized in several hybrid GNNs, which combine traditional message passing with the geometric scattering transform Wenkel et al. [2022], Min et al. [2022]. Similar to our method, these previous works essentially allow the model to apply different aggregation schemes at every node in a data-driven way. However, our method differs from the previous work by computing  $\bar{s}_f^{\text{low}}$  and  $\bar{s}_f^{\text{band}}$  separately, effectively *decoupling* the low-pass and band-pass filtering. By contrast, Wenkel et al. [2022] and Min et al. [2022] computing all of the  $s_f$ 's together in Equation 7.

In this section, we will provide a theoretical analysis of the advantages of our novel, decoupled attention mechanism. For clarity, we will refer to our method as the *decoupled hybrid block* and to the method from Wenkel et al. [2022] and Min et al. [2022] as the *non-decoupled hybrid block*.

To understand the decoupled hybrid block, we note that the low-pass filters  $F_k$  and band-pass filters  $F_{k_1, k_2}$  constitute fundamentally different operations and capture different types of information. While low-pass filters use a weighted averaging of the features of the nodes neighbors, band-pass filters *compare* two such averages of neighborhoods at different scale. As different types of information may be useful at different nodes, it is important that our MLP has access to both families of filterings.

However, we find that when grouped together, the outputs of the low-pass filters tend to be on a larger scale than the band-pass filters. Therefore, it is difficult for the MLP to extract band-pass information in the non-decoupled architecture. In the remainder of this section, we prove a theorem illustrating this phenomenon in certain circumstances as a complement to our empirical work showing that the decoupled architecture improves performance.

**Definition 1** (Minimal Filter Scale). For a band-pass filter  $F_{k_1, k_2}$  defined as in (5), we refer to  $k_{\min} := \min\{k_1, k_2\}$  as its minimal scale denoted  $\text{MS}(F_{k_1, k_2})$ . Similarly, for a low-pass filter  $F_k$  defined as in (4), we refer to  $k$  as its minimal scale and write  $\text{MS}(F_k) = k$ . For a filter bank  $\mathcal{F}$  consisting of multiple filters of the form  $F_k$  and  $F_{k_1, k_2}$ , we define the *minimal scale of the filter bank* to be smallest minimal scale of any of the filters, i.e.,  $\text{MS}(\mathcal{F}) := \min_{f \in \mathcal{F}} \{\text{MS}(f)\}$ .

**Definition 2** ( $c$ -balanced representation). Consider a non-decoupled attention mechanism as discussed. For  $0 < c < \infty$ , we say that the normalized scores are  $c$ -balanced at a vertex  $v$  if

$$\sum_{f \in \mathcal{F}_{\text{band}}} \bar{s}_f(v) = c \sum_{f \in \mathcal{F}_{\text{low}}} \bar{s}_f(v).$$

We may now state our theorem showing that in the non-decoupled architecture, the low-pass information will dominate the band-pass information, which helps explain the improved performance of the decoupled architecture. For a proof, and a more precise statement, please see Appendix A.

**Theorem 1.** *Consider a block of our network with a non-decoupled attention mechanism. If the minimal filter scale in each filter bank is sufficiently large, and the attention scores  $\bar{s}_f(v)$  are  $c$ -balanced at a vertex  $v$  for a moderate value of  $c$ , then low-pass filter responses at  $v$  will be at a much larger scale than the band-pass filter responses at  $v$ .*

## 6 Experiments

**Data & Benchmarks:** Our choice of benchmark datasets is based on those used in previous works exploring GNNs for CO problems [Karalias and Loukas, 2020, Zhang et al., 2023, Sun et al., 2022]. For the maximum clique problem, use the RB model from Xu et al. [2007] to generate challenging synthetic graphs as proposed by Karalias and Loukas [2020]. For MDS and maximum cut, we follow Zhang et al. [2023] and [Sun et al., 2022], generating Barabási–Albert (BA) graphs [Barabási and Albert, 1999] on *small* (200-300 vertices) and *large* (800-1200 vertices) scales.

For benchmarks, we use Gurobi [Gurobi Optimization, LLC, 2023], a state-of-the-art program solver that outperforms all deep learning-based methods in Karalias and Loukas [2020] and Zhang et al. [2023], alongside two heuristic approaches (Greedy and MFA) [Bilbro et al., 1988] and deep-learning

based solvers. We note that while Gurobi is very accurate when given large amounts of time, on tighter time budgets Gurobi is unable to find close-to-optimal solutions quickly [Karalias and Loukas, 2020]. As for deep-learning based solvers, we again compare our method against Karalias and Loukas [2020] (Erdős), Zhang et al. [2023] (GFN) and Sun et al. [2022] (Anneal). Erdős represents our main benchmark, i.e. the benchmark our model & training framework is most analogous to in that it is also a GNN-based encoder-decoder framework. Anneal represents a different avenue in that it proposes a novel training framework with an annealed loss function, while borrowing Erdős’ architecture directly. GFN is a powerful generative flow network [Bengio et al., 2021] based solver that represents the state-of-the-art deep learning method on various problems, albeit is considerably less scalable than GNN-based solvers.

The generated datasets in Zhang et al. [2023] are not directly available in the public domain: As a result, though we generate our datasets with identical procedures, we do not have access to the exact graphs used in previous work. Thus for fairer estimates, we evaluate our models using 5-fold cross-validation. As input node features to the Hybrid-CO GNN on synthetic graphs, we compute a collection of node-level statistics; we find that this approach is superior to using one-hot encodings (akin to Erdős/Anneal) or random features. For BA datasets we use node degree, eccentricity, cluster coefficient and triangle counts; we drop eccentricity on RB graphs due to its computational cost.

Table 1: Performance comparison of Hybrid-CO GNN with other baselines *small* datasets. Average of three runs with standard deviation listed. Best deep learning-based method highlighted in **bold**.

Method	Type	MCut size $\uparrow$ BA-small	Time $\downarrow$	MC size $\uparrow$ RB-small	Time $\downarrow$	MDS size $\downarrow$ BA-small	Time $\downarrow$
GUROBI	OR	732.47	13:04	19.05	1:55	27.89	1:47
GREEDY	H	688.31	0:13	13.53	0:25	37.39	2:13
GFN	SSL	704.30	2:57	<b>16.24</b>	0:42	<b>28.61</b>	2:20
ANNEAL	SSL	696.73	0:45	14.10	0:41	29.24	1:01
ERDÖS	SSL-GNN	693.45	0:46	12.02	0:41	30.68	1:00
Hybrid-CO GNN (Ours)	SSL-GNN	<b>724.21 <math>\pm</math> 0.49</b>	0:21	15.21 $\pm$ 0.21	3:08	30.17 $\pm$ 0.20	0:35

Table 2: Performance comparison of Hybrid-CO GNN with other baselines on *large* datasets. Average of three runs with standard deviation listed. Best deep learning-based method highlighted in **bold**.

Method	Type	MCut size $\uparrow$ BA-large	Time $\downarrow$	MC size $\uparrow$ RB-large	Time $\downarrow$	MDS size $\downarrow$ BA-large	Time $\downarrow$
GUROBI	OR	2915.29	1:05:29	33.89	16:40	103.80	13:48
GREEDY	H	2761.06	3:07	26.71	0:25	140.52	35:01
MFA	H	2833.86	7:16	27.94	2:19	126.56	36:31
GFN	SSL	2864.61	21:20	<b>31.42</b>	4:50	<b>110.28</b>	32:12
ANNEAL	SSL	2863.23	2:48	27.46	2:16	111.50	3:55
ERDÖS	SSL-GNN	2870.34	2:49	25.43	2:16	116.76	3:56
Hybrid-CO GNN (Ours)	SSL-GNN	<b>2954.72 <math>\pm</math> 0.68</b>	0:21	25.97 $\pm$ 0.29	4:10	114.74 $\pm$ 2.50	2:53

Table 3: Ablation study comparing our new decoupled layer to the non-decoupled version and common on message-passing layers from the literature for the MCut problem on BA-small dataset. Average of three runs with standard deviation listed.

Convolution	MCut size $\uparrow$
Hybrid-CO GNN (ours, decoupled)	<b>724.21 <math>\pm</math> 0.49</b>
Hybrid-CO GNN (ours, non-decoupled)	721.45 $\pm$ 1.99
GCN [Kipf and Welling, 2016]	717.15 $\pm$ 0.53
GIN [Xu et al., 2018]	716.23 $\pm$ 5.09

**Results & Analysis:** In Tables 1 and 2, we report the mean result of the objective sizes, in addition to inference times for *small* and *large* datasets respectively. OR refers to algorithmic solvers, H refers to heuristic methods while SSL refers to the self-supervised learning algorithms we compete against. All baseline results and notation in the two tables are as reported in from Zhang et al. [2023]. We report our results as mean  $\pm$  std. However, standard deviations were not reported for the baseline methods in Zhang et al. [2023].



Our Hybrid-CO GNN attains the most striking results for the maximum cut problem (MCut). In both BA-small and BA-large benchmarks, we obtain the new state-of-the-art results by a comfortable margin amongst all non-OR methods: On BA-small, we obtain a max cut size of 724.21: Almost 20 more than the next best result of the GFlowNet, and a mere 1.13% short of the Gurobi solver. We do so while also being by and large the fastest deep-learning based method, second only to the Greedy heuristic method amongst all benchmarks. On BA-large, the results are arguably even more impressive: We not only attain the best result amongst non-OR methods, but also surpass the Gurobi solver and establish a new SotA baseline. The success of Hybrid-CO GNN is further underlined by the fact that the inference time is largely invariant to the growing graph sizes, taking just 22 seconds to evaluate on 500 graphs – for comparison, it takes the Gurobi solver more than an hour to do so.

On the maximum clique (MC) and minimum dominating set (MDS) benchmarks, we obtain somewhat more modest but still very competitive results, and in particular outperform Erdős on every benchmark. On the MC benchmark RB-small, we demonstrate substantial improvements on Erdős and Anneal, while on the MDS benchmark BA-small we also improve on Erdős; in both sets of experiments our results either beat or are on par with the heuristic approaches, but fall short of Gurobi and GFN. The iterative GFlowNet algorithm proves particularly useful for these two tasks where GFN is the best SSL method by a comfortable margin. On the corresponding -large benchmarks, the results are largely similar: We improve on Erdős on both tasks and the heuristic methods for MDS-BA-large, but are outperformed on both by GFN and Anneal.

We thus emphasize here that our work is more directly comparable to the Erdős, the only GNN-based method with a focus on architectural components (as Anneal’s novelty is largely within its optimization framework rather than the MPNN architecture). By outperforming it on all benchmarks tested on, we demonstrate the power of Hybrid-CO GNN as a model framework for a wide array of graph-CO problems.

Finally, we performed an ablation study on the message-passing layers in order to demonstrate the architectural gains of the Hybrid-CO GNN layer compared to both previous scattering-based approaches and conventional MPNN layers, presented in Table 3. We compare our model with a variant of our proposed architecture *without* the decoupled filter bank and to two well-established baseline MPNNs, GCN [Kipf and Welling, 2016] and GIN [Xu et al., 2018], the latter of which forms the backbone of the Erdős’ GNN architecture. We use identical depth, width and training procedure for all models. Even when using the non-decoupled new architecture, we observe a clear improvement of more than 4 edges of the size of the cut on average compared to the best MPNN baseline (GCN) due to the introduced hybrid layer. Further, decoupling the filter bank improves the size by additional 3 edges. Similar to the Erdős’ GNN, we use skip-connections and batch normalization between layers, and perform minimal hyperparameter tuning, tuning only the number of message-passing layers. More details regarding hyperparameter tuning is available in Appendix B.

## 7 Conclusion

We have introduced a novel GNN which uses sophisticated pair of decoupled filter banks and a localized attention mechanism for solving several well-known CO problems. Our model can be trained in self-supervised fashion using loss functions  $L(\mathbf{p})$ , which allow us to estimate the probability  $\mathbf{p}(v)$  that each node is in the set of interest and then we utilize rule-based decoders in order to determine our solution. We then demonstrate the effectiveness of our method compared to a variety of common GNNs and other methods, obtaining new SotA baselines for the max cut problem. We note that in the future, it would be interesting to (a) combine our architectural improvements with better optimization frameworks to leverage the power of our model better, and (b) extend our method to other CO problems such as computing the graph coloring number. The primary challenge regarding the latter would be to develop either a suitable self-supervised loss function, or a computationally efficient method of producing labeled data to allow a supervised approach.

**Limitations and future work.** We observed that on the datasets with larger graphs, Hybrid-CO GNN was more difficult to optimize well, and demonstrated additional variance between runs compared with the small-dataset counterparts. This insight, alongside the particular success of Anneal on the -large datasets, directly points to the aforementioned phenomenon that the self-supervised loss functions associated with graph-CO problems are highly non-convex and difficult to optimize well. This however paves the way to an immediately relevant and promising future work: It is very likely

that by incorporating Hybrid-CO GNN in the annealed optimization framework proposed by Sun et al. [2022], we can arrive at a stronger framework across all tasks and datasets.

## Acknowledgments and Disclosure of Funding

This work was partially funded by the Fin-ML CREATE scholarship (PhD) and J.A. DeSève scholarship (PhD) [F.W.], Bourse en intelligence artificielle des Études supérieures et postdoctorales (ESP) 2023-2024 (PhD) [S.C.], FRQNT grant 299376, NSERC Discovery grant 03267, Canada CIFAR AI Chair, NIH (National Institutes of Health) grant NIGMS-R01GM135929 [G.W.], and NSF DMS grant 2327211 [G.W.,M.P.] The content provided here is solely the responsibility of the authors and does not necessarily represent the official views of the funding agencies.

## References

- Sergi Abadal, Akshay Jain, Robert Guirado, Jorge López-Alonso, and Eduard Alarcón. Computing graph neural networks: A survey from algorithms to accelerators. *ACM Computing Surveys (CSUR)*, 54(9):1–38, 2021.
- Albert-László Barabási and Réka Albert. Emergence of scaling in random networks. *Science*, 286(5439):509–512, 1999. doi: 10.1126/science.286.5439.509. URL <https://www.science.org/doi/abs/10.1126/science.286.5439.509>.
- Emmanuel Bengio, Moksh Jain, Maksym Korablyov, Doina Precup, and Yoshua Bengio. Flow network based generative models for non-iterative diverse candidate generation. In M. Ranzato, A. Beygelzimer, Y. Dauphin, P.S. Liang, and J. Wortman Vaughan, editors, *Advances in Neural Information Processing Systems*, volume 34, pages 27381–27394. Curran Associates, Inc., 2021. URL [https://proceedings.neurips.cc/paper\\_files/paper/2021/file/e614f646836aaed9f89ce58e837e2310-Paper.pdf](https://proceedings.neurips.cc/paper_files/paper/2021/file/e614f646836aaed9f89ce58e837e2310-Paper.pdf).
- Griff Bilbro, Reinhold Mann, Thomas Miller, Wesley Snyder, David van den Bout, and Mark White. Optimization by mean field annealing. In D. Touretzky, editor, *Advances in Neural Information Processing Systems*, volume 1. Morgan-Kaufmann, 1988. URL [https://proceedings.neurips.cc/paper\\_files/paper/1988/file/ec5decca5ed3d6b8079e2e7e7bacc9f2-Paper.pdf](https://proceedings.neurips.cc/paper_files/paper/1988/file/ec5decca5ed3d6b8079e2e7e7bacc9f2-Paper.pdf).
- A. Bojchevski and S. Günnemann. Deep gaussian embedding of graphs: Unsupervised inductive learning via ranking. In *Proc. of ICLR*, 2018.
- Shaked Brody, Uri Alon, and Eran Yahav. How attentive are graph attention networks? In *International Conference on Learning Representations*, 2021.
- Ronald R Coifman and Mauro Maggioni. Diffusion wavelets. *Applied and computational harmonic analysis*, 21(1):53–94, 2006.
- Austin Derrow-Pinion, Jennifer She, David Wong, Oliver Lange, Todd Hester, Luis Perez, Marc Nunkesser, Seongjae Lee, Xueying Guo, Brett Wiltshire, et al. Eta prediction with graph neural networks in google maps. In *Proceedings of the 30th ACM International Conference on Information & Knowledge Management*, pages 3767–3776, 2021.
- Matthias Fey and Jan E. Lenssen. Fast graph representation learning with PyTorch Geometric. In *ICLR Workshop on Representation Learning on Graphs and Manifolds*, 2019.
- Fernando Gama, Alejandro Ribeiro, and Joan Bruna. Diffusion scattering transforms on graphs. In *International Conference on Learning Representations*, 2018.
- Feng Gao, Guy Wolf, and Matthew Hirn. Geometric scattering for graph data analysis. In *International Conference on Machine Learning*, pages 2122–2131. PMLR, 2019.
- Gurobi Optimization, LLC. Gurobi Optimizer Reference Manual, 2023. URL <https://www.gurobi.com>.

- William L Hamilton, Rex Ying, and Jure Leskovec. Inductive representation learning on large graphs. In *Proceedings of the 31st International Conference on Neural Information Processing Systems*, pages 1025–1035, 2017.
- J. J. Hopfield and D. W. Tank. “neural” computation of decisions in optimization problems. *Biological Cybernetics*, 52(3):141–152, Jul 1985. ISSN 1432-0770. doi: 10.1007/BF00339943. URL <https://doi.org/10.1007/BF00339943>.
- Nikolaos Karaliyas and Andreas Loukas. Erdos goes neural: an unsupervised learning framework for combinatorial optimization on graphs. *Advances in Neural Information Processing Systems*, 33: 6659–6672, 2020.
- Richard Karp. Reducibility among combinatorial problems. volume 40, pages 85–103, 01 1972. ISBN 978-3-540-68274-5. doi: 10.1007/978-3-540-68279-0\_8.
- Thomas N. Kipf and Max Welling. Semi-supervised classification with graph convolutional networks. In *the 4th International Conference on Learning Representations (ICLR)*, 2016.
- Ilya Loshchilov and Frank Hutter. SGDR: stochastic gradient descent with restarts. *CoRR*, abs/1608.03983, 2016. URL <http://arxiv.org/abs/1608.03983>.
- Ilya Loshchilov and Frank Hutter. Fixing weight decay regularization in adam. *CoRR*, abs/1711.05101, 2017. URL <http://arxiv.org/abs/1711.05101>.
- Yimeng Min, Frederik Wenkel, Michael Perlmutter, and Guy Wolf. Can hybrid geometric scattering networks help solve the maximum clique problem? *Advances in Neural Information Processing Systems*, 35:22713–22724, 2022.
- Michael Perlmutter, Alexander Tong, Feng Gao, Guy Wolf, and Matthew Hirn. Understanding graph neural networks with generalized geometric scattering transforms. *SIAM Journal on Mathematics of Data Science*, 5(4):873–898, 2023.
- Haoran Sun, Etash K. Guha, and Hanjun Dai. Annealed training for combinatorial optimization on graphs, 2022.
- Alexander Tong, Frederik Wenkel, Dhananjay Bhaskar, Kincaid Macdonald, Jackson Grady, Michael Perlmutter, Smita Krishnaswamy, and Guy Wolf. Learnable filters for geometric scattering modules. *arXiv preprint arXiv:2208.07458*, 2022.
- Jan Tönshoff, Martin Ritzert, Hinrikus Wolf, and Martin Grohe. RUN-CSP: unsupervised learning of message passing networks for binary constraint satisfaction problems. *CoRR*, abs/1909.08387, 2019. URL <http://arxiv.org/abs/1909.08387>.
- Petar Velickovic, Guillem Cucurull, Arantxa Casanova, Adriana Romero, Pietro Lio, Yoshua Bengio, et al. Graph attention networks. *stat*, 1050(20):10–48550, 2017.
- Zichen Wang and Vassilis N. Ioannidis. How aws uses graph neural networks to meet customer needs, 2022. URL <https://www.amazon.science/blog/how-aws-uses-graph-neural-networks-to-meet-customer-needs>.
- Frederik Wenkel, Yimeng Min, Matthew Hirn, Michael Perlmutter, and Guy Wolf. Overcoming oversmoothness in graph convolutional networks via hybrid scattering networks. *arXiv preprint arXiv:2201.08932*, 2022.
- Shiwen Wu, Fei Sun, Wentao Zhang, Xu Xie, and Bin Cui. Graph neural networks in recommender systems: a survey. *ACM Computing Surveys*, 55(5):1–37, 2022.
- Ke Xu, Frédéric Boussemart, Fred Hemery, and Christophe Lecoutre. Random constraint satisfaction: Easy generation of hard (satisfiable) instances. *Artificial Intelligence*, 171(8):514–534, 2007. ISSN 0004-3702. doi: <https://doi.org/10.1016/j.artint.2007.04.001>. URL <https://www.sciencedirect.com/science/article/pii/S0004370207000653>.
- Keyulu Xu, Weihua Hu, Jure Leskovec, and Stefanie Jegelka. How powerful are graph neural networks? In *International Conference on Learning Representations*, 2018.

Jiaxuan You, Rex Ying, and Jure Leskovec. Design space for graph neural networks. In *NeurIPS*, 2020.

Dinghui Zhang, Hanjun Dai, Nikolay Malkin, Aaron Courville, Yoshua Bengio, and Ling Pan. Let the flows tell: Solving graph combinatorial optimization problems with gflownets. *arXiv preprint arXiv:2305.17010*, 2023.

Dongmian Zou and Gilad Lerman. Graph convolutional neural networks via scattering. *Applied and Computational Harmonic Analysis*, 49(3):1046–1074, 2020.

## A Proof of Theorem 1

The following is a more precise statement of Theorem 1.

**Theorem 2.** *Consider a block of our network with a non-decoupled attention mechanism. If the minimal filter scale in each filter bank is sufficiently large, and the attention scores  $\bar{s}_f(v)$  are  $c$ -balanced at a vertex  $v$  for a moderate value of  $c$ , then low-pass filter responses at  $v$  will be at a much larger scale than the band-pass filter responses at  $v$ .*

*More specifically, assume that we choose our graph shift operator as  $\mathbf{S} = \mathbf{P}$ , the lazy random walk matrix. Let  $v \in V$  be fixed and consider a single layer of the network with filter bank  $\mathcal{F} = \mathcal{F}_{\text{low}} \cup \mathcal{F}_{\text{band}}$ . Assume the non-linearity  $\sigma$  is non-negative and non-expansive, i.e.  $\sigma(x-y) \leq |\sigma(x) - \sigma(y)|$ . Assume that we have a single input feature  $\mathbf{x} \in \mathbb{R}^{n \times 1}$  which is entrywise non-negative and normalized so that  $\|\mathbf{x}\|_1 = 1$ . Let  $\mathbf{d} = A\mathbf{1}_n$  denote the degree vector.*

*Then, for all  $0 < \epsilon < \frac{\mathbf{d}(v)}{\|\mathbf{d}\|_1}$ , there exists  $K \in \mathbb{N}$  such that if  $MS(\mathcal{F}) \geq K$ , and the attention scores  $\{\bar{s}_f\}_{f \in \mathcal{F}}$  are  $c$ -balanced, we have*

$$\sum_{f \in \mathcal{F}_{\text{band}}} \bar{s}_f(v) \mathbf{H}_f(v) \leq \frac{c}{\frac{\mathbf{d}(v)}{\|\mathbf{d}\|_1} - \epsilon} \left( \sum_{f \in \mathcal{F}_{\text{low}}} \bar{s}_f(v) \mathbf{H}_f(v) \right) \epsilon.$$

*Proof.* Let  $v \in V$ , let  $0 < \epsilon < \frac{\mathbf{d}(v)}{\|\mathbf{d}\|_1}$ , and let  $\tilde{\mathbf{d}} = \frac{\mathbf{d}}{\|\mathbf{d}\|_1}$  denote the  $\ell^1$ -normalized degree vector. Since  $\mathbf{x}$  is entrywise non-negative and  $\ell^1$  normalized, we may interpret  $\mathbf{x}$  as a probability distribution. Therefore, since  $\mathbf{P}$  is the transition matrix of a lazy random walk, we have

$$\lim_{k \rightarrow \infty} \mathbf{P}^k \mathbf{x}(v) = \tilde{\mathbf{d}}(v).$$

Therefore, there exists  $K \in \mathbb{N}$  such that for  $k, k_1, k_2 \geq K$ , we have

$$\mathbf{P}^k \mathbf{x}(v) \geq \tilde{\mathbf{d}}(v) - \epsilon, \quad \text{and} \quad |(\mathbf{P}^{k_2} - \mathbf{P}^{k_1})\mathbf{x}(v)| \leq \epsilon.$$

Since in Section 5.1 we assume that  $m(\mathbf{x}) = \mathbf{x}$  or  $\mathbf{x} = \mathbf{x}$ , the assumption that each nonlinearity  $\sigma$  is nonexpansive and non-negative implies that if  $MS(\mathcal{F}) \geq K$  we have

$$\mathbf{H}_f(v) \geq \tilde{\mathbf{d}}(v) - \epsilon \geq 0, \quad \text{for all } f \in \mathcal{F}_{\text{low}}$$

and

$$0 \leq \mathbf{H}_f(v) \leq \epsilon, \quad \text{for all } f \in \mathcal{F}_{\text{band}}.$$

Therefore,

$$\sum_{f \in \mathcal{F}_{\text{low}}} \bar{s}_f(v) \mathbf{H}_f(v) \geq (\tilde{\mathbf{d}}(v) - \epsilon) \sum_{f \in \mathcal{F}_{\text{low}}} \bar{s}_f(v)$$

and

$$\sum_{f \in \mathcal{F}_{\text{band}}} \bar{s}_f(v) \mathbf{H}_f(v) \leq \epsilon \sum_{f \in \mathcal{F}_{\text{band}}} \bar{s}_f(v).$$

Combining the previous two inequalities yields

$$\begin{aligned} \sum_{f \in \mathcal{F}_{\text{band}}} \bar{s}_f(v) \mathbf{H}_f(v) &\leq \frac{\epsilon}{\tilde{\mathbf{d}}(v) - \epsilon} \left( \frac{\sum_{f \in \mathcal{F}_{\text{band}}} \mathbf{s}_f(v)}{\sum_{f \in \mathcal{F}_{\text{low}}} \mathbf{s}_f(v)} \right) \sum_{f \in \mathcal{F}_{\text{low}}} \bar{s}_f(v) \mathbf{H}_f(v) \\ &= \frac{c}{\tilde{\mathbf{d}}(v) - \epsilon} \left( \sum_{f \in \mathcal{F}_{\text{low}}} \bar{s}_f(v) \mathbf{H}_f(v) \right) \epsilon. \end{aligned}$$

□

## B Experimental setup & hyperparameters

Our experimental framework is built on PyTorch Geometric [Fey and Lenssen, 2019] and Graph-Gym [You et al., 2020]. All experiments are conducted using a single GPU and 4 CPUs; most experiments (e.g. MC experiments on -small graphs) ran within several minutes to an hour, while the largest (e.g. MDS on BA-large using 16-layer-256-width Hybrid-CO GNN) took several hours to converge.

We perform all timing experiments in Tables 1 and 2 following the setup in Zhang et al. [2023], using an NVIDIA V100 GPU for fair comparison of the inference time estimates on 500 samples. We report worst-case results, i.e. use a batch size of 1; assuming that Zhang et al. [2023] have done so despite not listing an explicit batch size for the timing experiments. Note that wall-clock time for Hybrid-CO GNN experiments for MCut on either dataset, for example, takes about 3 seconds if a batch size of 256 is used.

As mentioned, the self-supervised loss functions associated with combinatorial graph problems are difficult to optimize well, due to their highly non-convex nature. We thus conducted hyperparameter optimization on several main components of our model. For each task, a separate set of hyperparameter tuning experiments were conducted for number of layers, layer width and activation, as well as L2 normalization for layers and LR where appropriate. As is the case with hyperparameter tuning, a considerable portion of the experiments did not make it to the final results.

In addition to the configurations listed in Table 4, all tasks used an AdamW optimizer Loshchilov and Hutter [2017] with a cosine annealing scheduler Loshchilov and Hutter [2016], with a 5-epoch warmup period for MCut and MDS tasks.

Table 4: Overview of model hyperparameters associated with the reported results for each dataset.

	<b>MCut BA-small</b>	<b>MCut BA-large</b>	<b>MC RB-small</b>	<b>MC RB-large</b>	<b>MDS BA-small</b>	<b>MDS BA-large</b>
<b># Layers</b>	16	16	8	8	16	16
<b>Layer width</b>	256	256	256	128	256	256
<b>Activation</b>	ELU	ELU	GELU	GELU	GELU	GELU
<b>L2 Normalization</b>	Yes	Yes	No	Yes	Yes	Yes
<b>LR</b>	3e-3	3e-3	1e-3	1e-3	3e-3	3e-3
<b># Epochs</b>	200	200	20	20	200	200

## C Transferability experiments

We have additionally conducted several experiments that demonstrate the ability of Hybrid-CO GNN to generalize to larger graphs than it was trained on. In Table 5, we tested our a Hybrid-CO GNNs trained on RB-small, BA-small and BA-small datasets for MC, MDS and MCut tasks respectively (Table 1) on the -large variants of each dataset. We then compared the results to the results of GNN-based models (ERDÖS, ANNEAL and Hybrid-CO GNN trained on {RB/BA}-large). We see that particularly for the max cut problem, Hybrid-CO GNN trained on the BA-small generalizes well to BA-large, surpassing all non-Hybrid-CO GNN methods, including GFN & GUROBI which are not listed here. For MC and MDS, we are unable to surpass other GNN methods, but are relatively close particularly on MDS, passing GREEDY & MFA from Table 2. These results are quite encouraging in that they demonstrate strong generalizability on relatively difficult synthetic graph-CO tasks, and implies that pre-training expressive GNN-based models such as Hybrid-CO GNN may be a powerful tool towards solving CO problems on large graphs.

Table 5: Performance comparison of Hybrid-CO GNN trained on {RB/BA}-small) to GNN-based benchmarks on {RB/BA}-large datasets.

<b>Model</b>	<b>Training dataset</b>	<b>MCut BA-large</b>	<b>MC RB-large</b>	<b>MDS BA-large</b>
ERDÖS	{RB/BA}-large	2870.34	25.43	116.76
ANNEAL	{RB/BA}-large	2863.23	27.46	111.50
Hybrid-CO GNN (Ours)	{RB/BA}-large	$2954.72 \pm 0.68$	$25.97 \pm 0.29$	$114.74 \pm 2.50$
Hybrid-CO GNN (Ours)	{RB/BA}-small	$2930.60 \pm 1.52$	$23.02 \pm 0.08$	$118.75 \pm 1.54$